Int. J. Electrochem. Sci., 7 **(2012)** 8676 - 8687

International Journal of
ELECTROCHEMICAL
SCIENCE
www.electrochemsci.org

Aqueous Additive for Lithium Ion Batteries: Promotes Novel Solid Electrolyte Interface (SEI) Layer with Overall Cost Reduction

Chin-Shu Cheng[1,2], *Fu-Ming Wang*[1,3,*], *John Rick*[1]

[1]Sustainable Energy Center, National Taiwan University of Science and Technology, Taipei, Taiwan
[2]Department of Chemical Engineering, National Tsing Hua University, Hsinchu, Taiwan
[3]Graduate Institute of Applied Science and Technology, National Taiwan University of Science and Technology, Taipei, Taiwan
[*]E-mail: mccabe@mail.ntust.edu.tw

Received: 23 July 2012 / *Accepted:* 15 August 2012 / *Published:* 1 September 2012

A novel technology, easily incorporated into the manufacturing process for lithium ion batteries, offers the prospect of significant performance improvements. Applying this technology, the manufacturing process can result in batteries with increased energy densities, which are able to supply markets where high energy/power requirements are demanded, such as in electric vehicles (EV). In this research, we show a moisture curing reaction mechanism, in which maleimide (MI) reacts with water and a lithium salt to form a temperature stable (55℃) three-dimensional nano tunnel in the solid electrolyte interface (SEI) on the carbon anode's surface, can be used for both performance enhancement and cost reduction. By using this binary additive (MI/H_2O), lithium ion batteries not only obtain a higher energy density, but their attendant manufacturing costs in terms of dry room electric power consumption and the storage costs associated with aging after manufacture are significantly reduced.

Keywords: Lithium ion battery, additive, water, solid electrolyte interface, maleimide.

1. INTRODUCTION

Lithium ion batteries have received considerable attention over the last two decades because of their high energy density [1-2]. Li batteries are fabricated in a low-humidity environment to prevent atmospheric moisture from reacting with the lithium ions in the electrolyte [3]. In addition, electrodes having excessively high water contents are also liable to undergo a gas liberating electrolysis reaction during operation [4]. According to the related literature [3-6], the lithium salt in the electrolyte is

dissociated according to the following two equations:

$$LiPF_6 \rightarrow Li^+ + PF_6^- \quad (1)$$

$$LiPF_6 \rightarrow LiF + PF_5 \quad (2)$$

However, the lithium single ion (Li^+) and the Lewis acid (PF_5) easily react with water to produce HF and other unwanted products. Therefore, water is conventionally regarded as being detrimental to lithium batteries. The following equations demonstrate the reactions that occur inside the lithium ion battery, leading to its inferior performance.

$$PF_5 + H_2O \rightarrow POF_3 + HF \quad (3)$$

$$POF_3 + H_2O \rightarrow POF_2OH + HF \quad (4)$$

$$H_2O + Li^+ + e^- \rightarrow LiOH + H_2 \quad (5)$$

$$LiOH + Li^+ + e^- \rightarrow Li_2O + H_2 \quad (6)$$

$$Li_2O + HF \rightarrow LiF + H_2O \quad (7)$$

Thus, the HF both degrades the crystalline lattice structure of the cathode and anode materials, and also attacks and decomposes the solid electrolyte interface (SEI) on the carbon anode's surface. In addition, ionic insulators i.e. POF_3, POF_2OH, Li_2O, LiF, LiOH, and Li_2CO_3, deposited on both electrodes' surfaces, inhibit ionic diffusion and the intercalation performance of lithium ions.

This paper demonstrates a new method that subverts the established view, by directly using water as an additive in lithium ion batteries to solve the above problems, while enhancing performance during high-temperature operation. The mixing system (MI/H_2O) is used here in a comprehensively novel approach to lithium ion battery production. We have also investigated the multiple interactions among MI, H_2O, lithium salts, SEI properties and their effects on battery performance.

2. EXPERIMENT

The graphite anode consisted of 93 wt % mesocarbon microbeads (MCMB-2528, Osaka Gas Corp., Japan), 3 wt % KS-4 as a conductive additive and 4 wt % poly(vinylidene)fluoride (PVDF, Kureha Chemical, Japan) as a binder. The cathode material was a formulation consisting of 91 wt % lithium cobalt oxide ($LiCoO_2$- L106 LICO Corp., Taiwan) as the active material, 5 wt % conductive carbon (KS-6, Showa, Japan) and 4 wt% poly(vinylidene)fluoride (PVDF, Kureha Chemical, Japan) as

a binder. The basic electrolyte used in this study was 1M lithium hexafluorophoshate ($LiPF_6$) dissolved in a mixture of ethylene carbonate (EC), propylene carbonate (PC), diethylene carbonate (DEC) (3:2:5 by volume, electrochemical grade from Ferro) and 2 wt % vinylene carbonate (VC).

N'N-1,4-phenylenedimaleimide [0.1 wt % (MI)], additionally containing H_2O (100 ppm), was completely dissolved in the multi-carbonate-based basic liquid electrolyte at room temperature and used as the primary organic, small molecular weight, additive. All the electrochemical measurements and SEM analyses were carried out according to previously reported literature procedures [7].

3. RESULTS AND DISCUSSION

According to our previous results [8], the electrolyte when combined with MI/H_2O can lead to substantial improvements in both the energy density and life cycle during high-temperature operation.

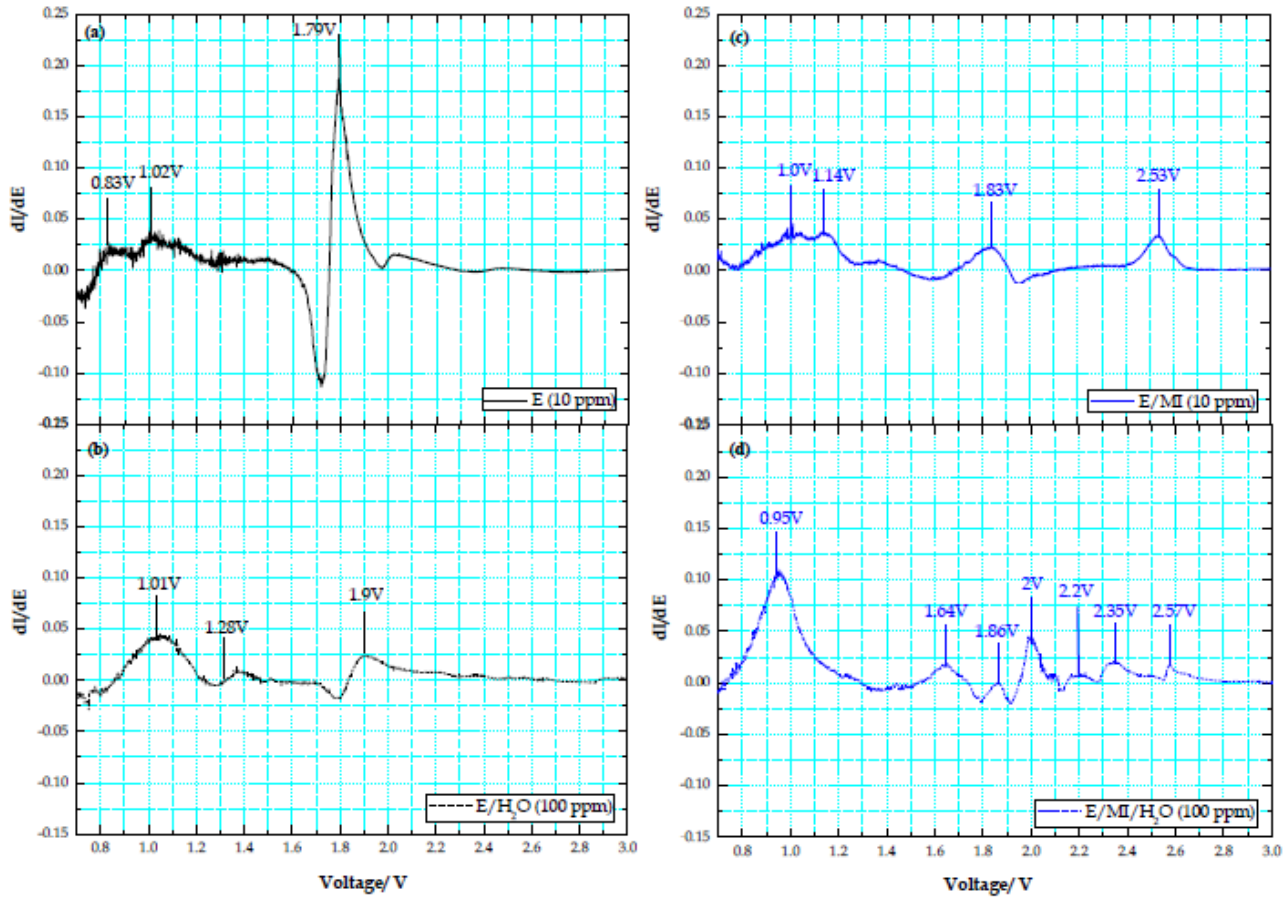

Figure 1. The differential cyclic voltammograms analysis of electrolytes without additive at (a) 10 ppm; (b) 100 ppm of water content and with MI additive at (c) 10 ppm; (d) 100 ppm. Working and counter electrode, stainless steel; reference electrode, lithium; scan rate is 0.1 mVs^{-1}

To better understand the relationship between the curing reaction and the SEI forming

mechanism with the MI/H_2O binary additive, differential cyclic voltammogram (CV) measurements were used to determine the reason for water not affecting the batteries performance. Fig. 1a shows three typical electrochemical current responses, of pure commercial electrolytes, containing less than 20 ppm water. These responses can be assigned to a vinylene carbonate (VC) reduction potential at 1.79 V and propyl/ethyl carbonate (EC/ PC) reduction potentials at 1.02 V/0.83 V. Fig. 1b shows that, after the water content increases to 100 ppm, an additional water reduction potential is assigned at 1.28 V. This is a typical hydrolysis potential of water, as mentioned in extant literature [9]. In the meantime, the potentials of VC and EC/PC shift to 1.9 V and 1.05 V, respectively - suggesting that water limits VC electrochemical reduction: note that the current density of all the responses is smaller than those shown in Fig. 1a.

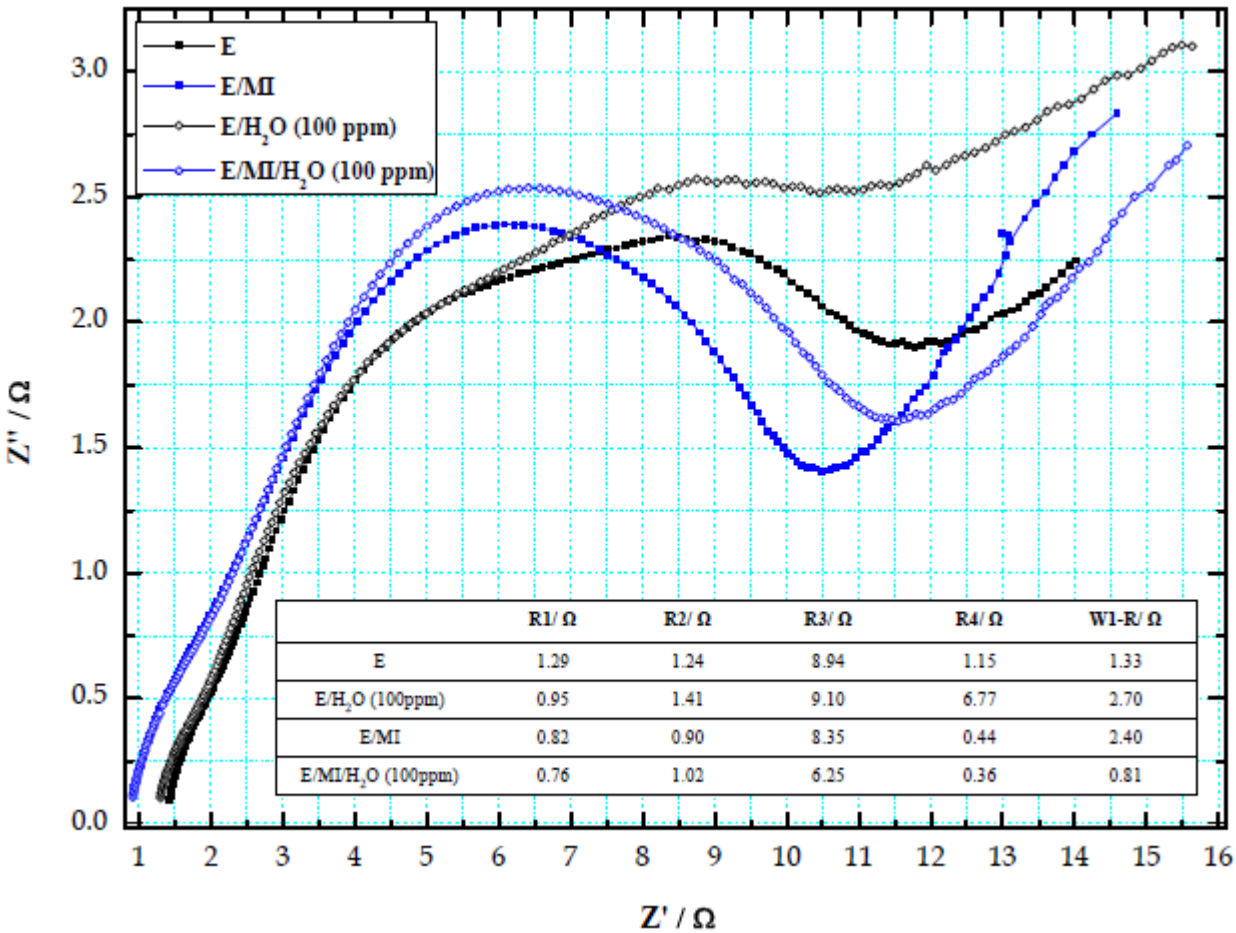

	R1/ Ω	R2/ Ω	R3/ Ω	R4/ Ω	W1-R/ Ω
E	1.29	1.24	8.94	1.15	1.33
E/H_2O (100ppm)	0.95	1.41	9.10	6.77	2.70
E/MI	0.82	0.90	8.35	0.44	2.40
E/MI/H_2O (100ppm)	0.76	1.02	6.25	0.36	0.81

Figure 2. Impedance Spectra of $LiCoO_2$/ MCMB full cell after 1st battery formation. Schematic representation of the item of equivalent circuit inside the $LiCoO_2$/MCMB battery has been arranged inside the figure.

Hence, the electrochemical reaction of the lithium ion battery does not require copious amounts of water. For comparison, Fig. 1c shows that when the primary additive (MI) was added into the electrolyte (specific reduction potential 2.53 V), with VC, EC, and PC, the resulting specific reduction potentials were 1.83 V, 1.14 V, and 1.0V, respectively. The curves indicate the electrochemical

behavior of each compound, and thus represent independent reactions of MI, VC, PC, EC, and H_2O. However, Fig. 1d shows differing results to other figures, in which MI promptly reacts with a lithium ion and water to form complex ligands, with specific reduction potentials, in the range of 1.6 V to 2.6 V. The first potential at 2.57 V is assigned to a portion of MI reduction, and the multiple responses at 2.35 V, 2.2 V, 2 V, and 1.86 V are the combined reaction of residual MI, lithium ions and H_2O. Finally, VC and EC/PC are assigned to 1.64 V and 0.95 V, respectively. Thus, this observation indicates that MI, lithium ions, and H_2O are fabricated to form an inner SEI on the electrode's surface duo to the higher reduction potential of the combined reaction. Other solvents, such as VC and EC/PC, formed an outer SEI behind the combined reaction product of the MI, lithium ions, and H_2O. We defined this as the 'core-shell double layer of SEI'. This innovative inner SEI enhances the transport properties of lithium ions and effectively maintains the batteries performance.

The AC impedance spectra of batteries with four different electrolytes are shown in Fig. 2. For comparison, the smaller blue hollow semicircles represent the lower impedance behavior when MI is added to the electrolyte. The secondary additive, H_2O, was added to combine with MI and is displayed by a smaller semicircle with a solid blue line, this indicates the lowest impedance of the battery. Riveted refinement of the equivalent circuit model was used to simulate and demonstrate the physical meanings of the four semicircles, identifying the internal construction of the battery. The table shown in Fig. 2 provides information on the simulation parameters. First, the primary additive, MI, was added to the electrolyte and decreased the electrolyte's resistance from 1.29 Ω to 0.82 Ω because of the four electron-withdrawing carboxyl (-C=O-) groups on the MI structure that assisted salt dissociation while offering high ionic electrolyte conductivity. A second, water addition increased the outer SEI resistance of the R_2 in 12% increments, from 1.24 Ω (E) to 1.41 Ω (E/H_2O) and 0.9 Ω (E/MI) to 1.02 Ω (E/MI/H_2O). This result demonstrates that MI, due to its higher reduction potential, does not participate in outer SEI formation. Therefore the composition and thickness of the outer SEI is not affected by the additional water which will react with a fixed amount of lithium ions to form an insulating layer on the electrode's surface, thereby eliminating the transport of lithium ions. In addition, R_3 is correlated to evidence of the moisture curing reactions of water with MI and lithium ions, because the value decreased by 25% from 8.35 Ω (E/MI) to 6.25 Ω (E/MI/H_2O). The inner SEI was clearly fabricated by MI, lithium ions, and water. By contrast, the insulators formed on the electrode's surface (without the MI primary additive) eradicated ionic transport and caused the resistance to increase from 8.94 Ω (E) to 9.10 Ω (E/H_2O). The R_3 values of E and E/MI also confirmed our previous assumption that the inner SEI results from the electron-withdrawing carboxyl (-C=O-) groups on the MI structure, and reduces the resistance from 8.94 Ω (E) to 8.35 Ω (E/MI). All R_3 results indicated that MI, lithium ions, and water in combination facilitate a high ionic conductive of SEI, thereby assisting the ionic diffusion and intercalation performance. R_4 represents the contact resistance (charge transfer resistance, R_{ct}) between the inner SEI and the electrode's surface. The AC result demonstrates that the ionic conductive of the SEI 'matures' efficiently on the carbon electrode's surface [10-12]; therefore, its contact resistance with the electrode surface is small, and produces a value of 0.36 Ω (E/MI/H_2O). However, when the electrolyte does not contain MI, the water reacts directly with lithium ions, and the reaction products (i.e. insulators) form over the electrode's surface increasing the resistance significantly to 6.77 Ω (E/H_2O). This 20-fold disparity in contact resistance

between E/MI/H_2O and E/H_2O indicates the importance of designing a suitable SEI for a lithium ion battery. Finally, Warburg analysis revealed that, despite the inner and outer SEI on the electrode's surface, the resistance (0.81 Ω) of the bulk electrodes with a binary additive is superior to that of electrodes with only water (2.70 Ω), which may be because of the higher reduction potential of complex combined reaction and the subsequent formation of the inner SEI significantly affecting both the cathode and anode. Thus, the ionic conductive of SEI reinforces the performance of Li^+ intercalation and de-intercalation performance to the cathode and anode materials.

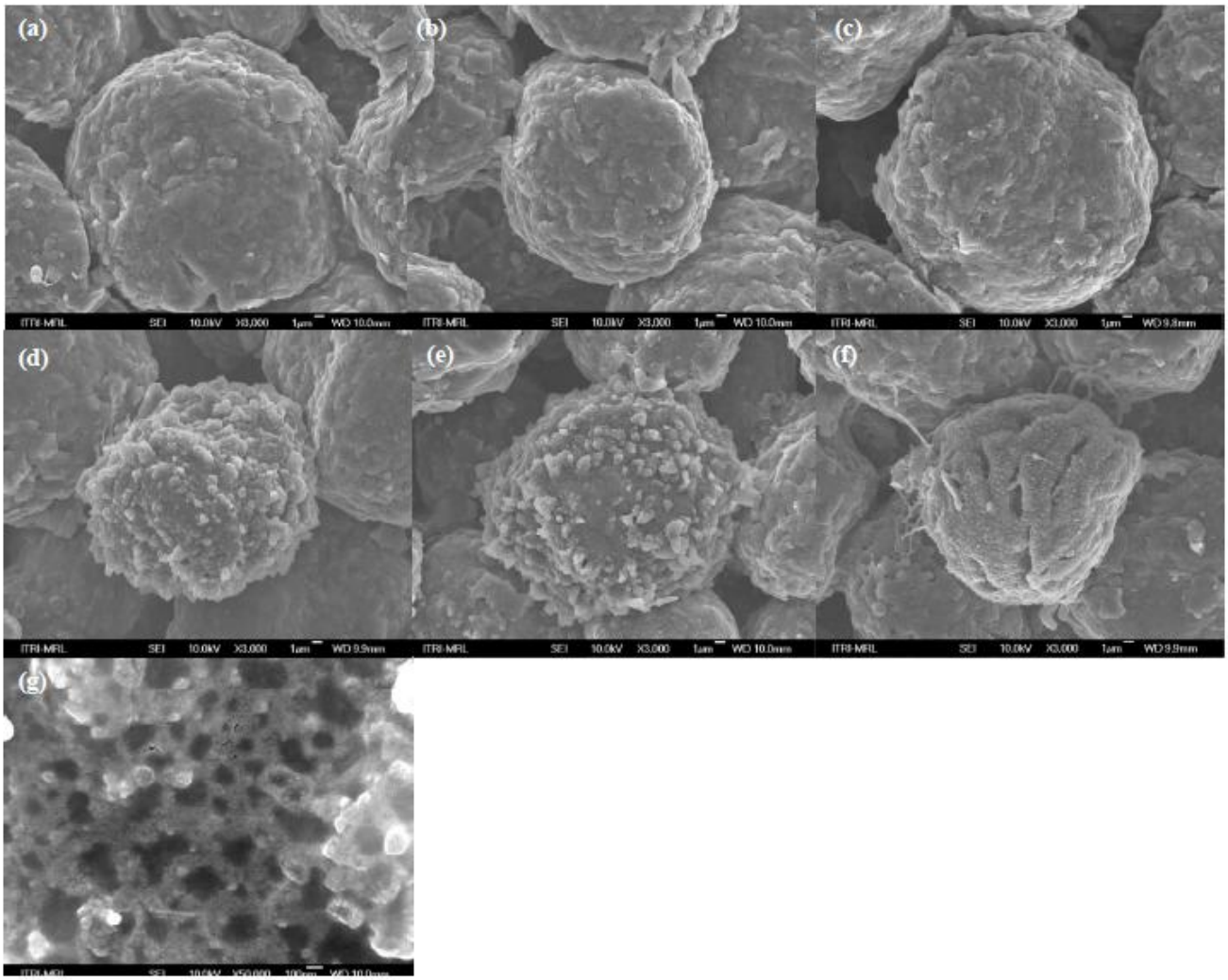

Figure 3. The SEM photographs of MCMB particle on the 3,000 scale without additive at (a) 10 ppm; (b) 100 ppm; (c) 250 ppm of water content and with MI additive at (d) 10 ppm; (e) 100 ppm; (f) 250 ppm after 35 cycles discharged on full cell. (g) The enlarge photograph of fig 4e on the 50,000 scale.

Figure 3 shows the SEM surface morphology of the MCMB anode, which was assembled from a full cell. Fig. 3a shows a ball-like particle of MCMB (25-30 μm in diameter); the flakes of the PVDF and the small pellets of KS-6 were homogeneously distributed on the graphite anode, which was

charged and discharged using a fresh commercial electrolyte (water content less than 20 ppm) after 35 cycles. When an additional amounts of water (100 ppm and 250 ppm) were added to the batteries, the morphologies shown in both photographs (Figs. 3b and 3c) became similar, indicating that water does not significantly influence the morphology of MCMB. Fig. 3d shows that MI added into the electrolyte, is similar to Fig. 3a. However, Fig. 3e shows several coral-like piles homogeneously distributed around the particle's surface. Furthermore, Fig. 3f shows a remarkable morphology because the MCMB particle was already covered with a thick and carpet-like SEI. Therefore, the SEM images verified that MI can react with lithium ions and water to fabricate a useful SEI. Fig. 3g displays an enlarged picture of Fig. 3e, showing that the SEI comprehensively 'honeycombed' the surface forming several 'caves' almost 100 nm in width. This particular phenomenon is referred to as a novel SEI layer with 3D ionic nano-tunnels for lithium ion batteries.

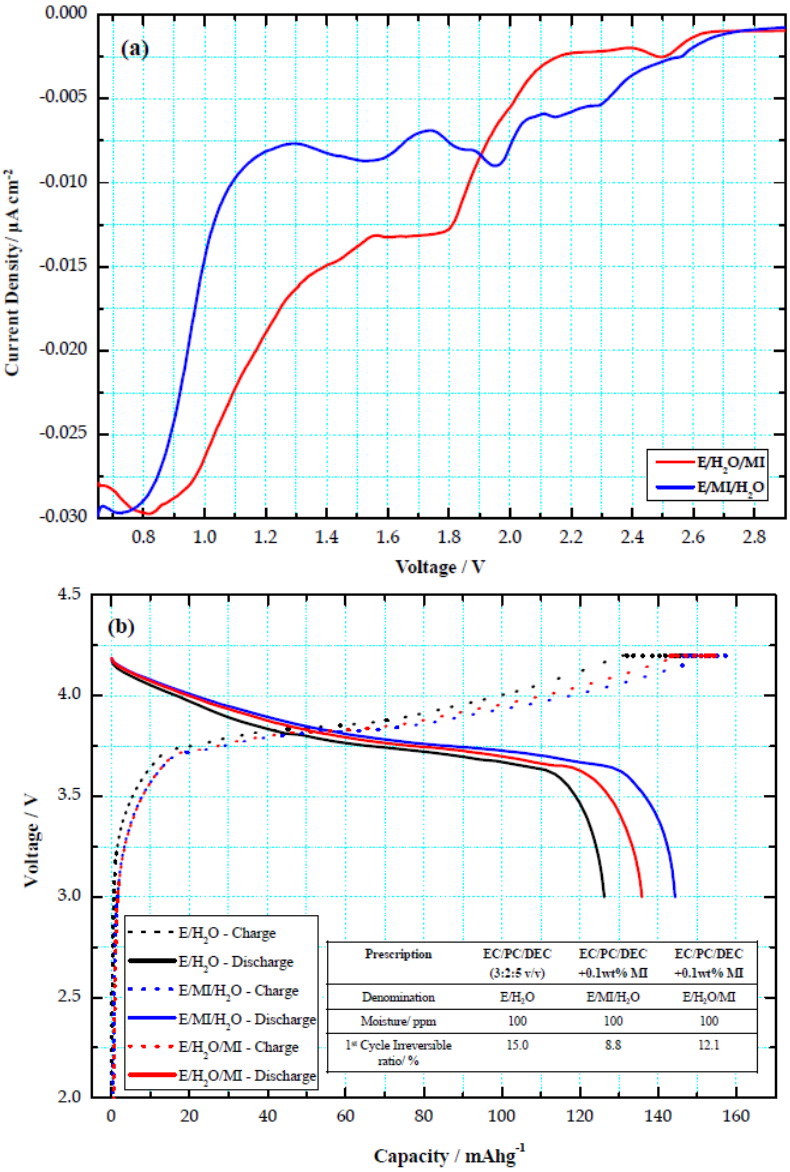

Figure 4. The electrochemical measurements regarding the comparisons of the additive addition sequence in electrolyte (a) The linear sweep voltammetry (LSV) analysis and (b) charging and discharging curves of battery formation at 0.1C/ 0.1C, irreversible ratio representation of the $LiCoO_2$/MCMB battery has been arranged inside the figure.

The authors have assumed that numerous reviewers may be confused with the effect of water on the electrochemical reaction, in which water first reacts with lithium ions that are dissociated from $LiPF_6$. According to related studies [3-6], H_2O must react with lithium ions and form ionic insulators, such as LiOH and further unnecessary compounds. The changes in sequence of additives in the experiments were demonstrated by linear sweep voltammogram (LSV) measurements to identify the reaction mechanism among MI, lithium salt, and water. The red line in Fig. 4a indicates that the fresh electrolyte contains a 1M concentration of lithium salts, to which 100 ppm of water was subsequently added. After stirring for 1 h, an additional 0.1 wt. % of MI was added to the electrolyte. This addition is defined as E/H_2O/MI. Based on the red LSV curve of this electrolyte; this paper offers four conclusions, as follows:

1. MI reduction takes place at 2.6-2.4 V and exhibits a slight current response as is expected from the small amount of concentration (0.1 wt. %) in the electrolyte.
2. Li ions react with H_2O during stirring leading to an increase in current density and insulator formation at approximately 2.0-1.0 V during LSV.
3. MI does not react with insulators that were formed by lithium ions and H_2O.
4. The reduction of carbonate based electrolytes take place below 1 V.

In addition, the blue line in Fig. 4a demonstrates that the fresh electrolyte initially contains a 1M concentration of lithium salts, to which 0.1 wt % of MI was added. After stirring for 1 h, 100 ppm of water was added to the electrolyte. The stage is denoted as E/MI/H_2O in the sequence. Based on the blue LSV curve, representing this electrolyte, we offer three additional conclusions, as follows:

1. MI reacted with lithium ions during stirring and produced a complex combination reaction, which facilitated multiple reduction responses at approximately 2.6-1.8 V during LSV measurement.
2. The H_2O subsequently reacted with the complex compounds, lithium based ligand, which was formed by Li ions and MI of the combination reaction, during stirring, to exhibit a broad but low intensity response at approximately 1.6-1.3 V.
3. Carbonate electrolyte reduced to below 1 V.

The primary additive proved that MI reacts with lithium ions during electrolyte stirring to form a lithium based ligand. This compound continues the electrochemical reaction with H_2O. Thus, a novel inner SEI is synthesized on the carbon anode's surface. By contrast, the inert insulators do not react with MI, with the LSV spectrum revealing the independent reduction of insulators, and not the complex multi-stage reaction shown by the lithium based ligand. For practical applications, the trade-off between battery performance and the electrolyte augmentation sequence was measured, as shown in Fig. 4b. The charge-discharge curves demonstrate that the lowest irreversible ratio (8.8%) of the first cycle of battery formation occurs when the MI is first added into the electrolyte, and provides an energy density of 143.6 $mAhg^{-1}$, which is higher than that the electrolyte with only 100 ppm of water (128.1 $mAhg^{-1}$) and the electrolyte with the addition of water first and MI second (138 $mAhg^{-1}$). This result confirms the conclusions of our previous experiments, in that the binary additive system (MI/H_2O) facilitates the lithium ion battery manufacturing process, while enhancing performance at high temperatures (approximately > 55 ℃); however, the final battery performance is determined by described sequential addition [8].

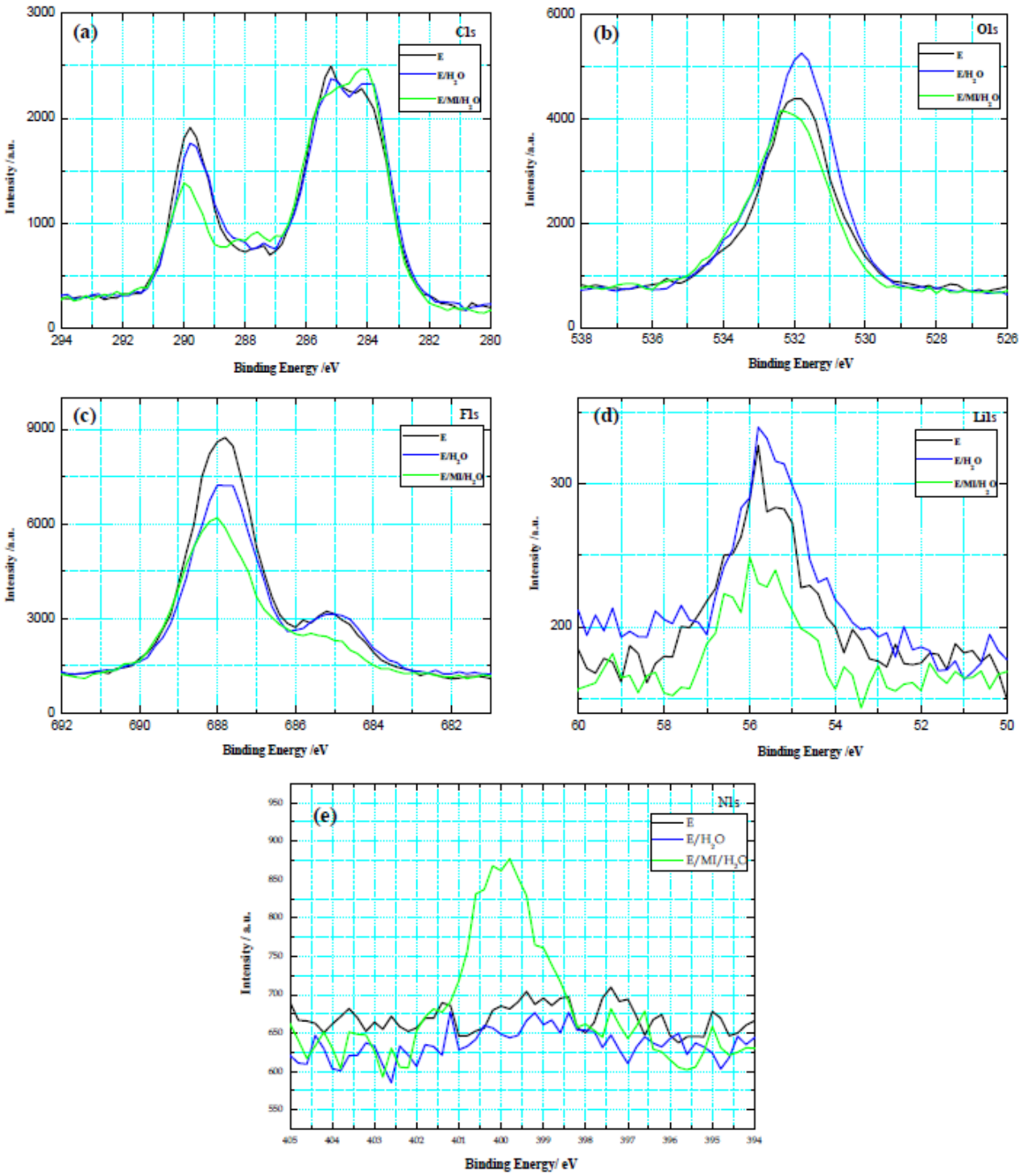

Figure 5. XPS analysis of (a) C1s, (b) O1s, (c) F1s, (d) Li1s and (e) N1s spectra on MCMB surface of electrode .

X-ray photoelectron spectroscopy (XPS) was used to ascertain the nature of the inner SEI, with the lithium based ligand, and determine the chemical composition of the SEI compared to pure electrolyte (E) and the electrolyte with additional water (100 ppm), i.e. E/H_2O. Fig. 5a shows a C1s spectrum, which can be divided into three regions. The first region 284~286 eV, represents the sp2 (-C-

C-) carbon structure at 284.4 eV [13] and the hydroxyl-carbon bonding (-C-OH-) of organic compounds at 285.5 eV [14] on the MCMB surface. The green line in Fig. 5a confirms that the SEI layer fabricated by E/MI/H_2O is thinner than the others (black and blue lines) because the -C-C- intensity signal is the highest on the carbon surface. In addition, previous studies [15-16] have indicated that hydrocarbon bonding at 285.5 eV usually originates in polymers from SEI. Thus, the amount of SEI due to the lithium-based ligand (by electrochemical transformation) is less than that of the other two. This figure also confirms that the amount of inorganic insulators (LiOH, Li_2O and Li_2CO_3) of the electrolyte of E/H_2O was less than E because the lithium ions react to H_2O, which weakens the hydrocarbon intensity. The second region was 286~288 eV, indicating -C-H- bonding of RCH_2OCO_2Li at 287.6 eV [17]. The primary additive of MI reacts with lithium ions and comprises lithium-based ligands. Such ligands subsequently react with H_2O to fabricate a three-dimensional nano tunnel SEI; therefore, the intensity of -C-H- bonding of RCH_2OCO_2Li was higher than that of the electrolytes of E and E/H_2O when their intensities are the same. This behavior verified our original concept of novel SEI formation with H_2O in lithium battery. The third region was identified to a -C-O- bonding of Li_2CO_3 at 289 eV [18] and a -C-O- bonding of RCH_2OCO_2Li (alkyl lithium carbonates) at 290 eV [14]. According to the position of 289 eV, the electrolytes of E and E/H_2O exhibited a higher amount of Li_2CO_3 than the electrolyte of E/MI/H_2O. This behavior represents the insulator formation that was previously introduced. In C1s spectrum, the electrolyte of E/MI/H_2O is approximately 15-20 nm, as determined by: sputtering measurements, organic composition, and ligand electrochemical polymerization of the thinner SEI layer. Fig. 5b shows two regions in the O1s spectrum that can be distinguished using 532.5 eV as a separating parameter. The first region at 526~532.5 eV displays the Li_2O, Li_2CO_3, and LiOH formations, which are assigned to 528.6, 532, and 531.9 eV, respectively [19]. This result confirms the conclusion of C1s, indicating that the insulators deposited on the carbon surface and the peak intensity of E/H_2O were stronger than E and E/MI/H_2O. We verified that MI is used to react with lithium ions and H_2O and inhibits the formation of insulators. According to the integral area analysis of O1s spectrum, Li_2O uses 10%, Li_2CO_3 uses 58% and LiOH uses 32% in the first region. The second region of 532.5 eV-538 eV exhibits an organic SEI formation, including -C-O- (532.5 eV) [14] and -C=O- (533.8 eV) [20] of RCH_2OCO_2Li structure. Hence, the intensity of -C-O- and -C=O- with the electrolyte of E/MI/H_2O is higher, and forms a high ionic conductivity of SEI layer. We cannot detect any $Li_xPF_yO_z$ formation at 535 eV [21] within three electrolyte prescriptions, indicating that the insulators on the carbon surface do not have $Li_xPF_yO_z$. Fig. 5c shows two typical areas of F1s spectrum. First, the non-dissociated lithium salt of $LiPF_6$ was detected at 688.8 eV [14], demonstrating a decrease of the combination of MI and salt, which ensures the peak intensity. In addition, the intensity of E/H_2O is higher than E/MI/H_2O, which indicates that the lithium ions reactivity with MI exceeds that of the lithium ions with H_2O. In addition, this figure verifies the results in Fig. 1. Second, the location of 685 eV describes LiF formation [14]. Similarly, the electrolyte of E/MI/H_2O confirms a smaller number of insulators of SEI on the carbon surface. Fig. 5d shows the spectrum of Li1s, and assigns Li_2CO_3 at 55.5 eV [22] and LiF at 56 eV [14], respectively. The spectrum intensity of E and E/H_2O was higher than that of E/MI/H_2O because of the previously stated reasons. However, remarkable behavior was noted at 56.6 eV with an electrolyte comprising E/MI/H_2O, namely the formation of a three-dimensional nano tunnel SEI, which we assumed may be

due to the lithium-based ligand. Fig. 5e shows an N1s spectrum of the MCMB surface, indicating that the three-dimensional nano tunnel SEI was fabricated by the MI, which exhibits a perspective -C-N- bonding at 400.3 eV [7], and also verifies the combination reaction of MI, lithium salt, and H_2O.

4. CONCLUSIONS

In conclusion, we used a novel binary additive system to verify that the combined use of maleimide (MI) as a primary additive in combination with H_2O as a secondary additive is a viable strategy to increase both the charge/discharge rate and cycling ability of lithium ion batteries. We successfully synthesized a three dimensional nano tunnel of SEI with a defined order of additives to optimize the properties of SEI, such as its chemical composition and mechanism of formation. Consistent with our electrochemical measurements, this novel binary additive retains its function on the carbon anode's surface. Although, the MI/H_2O binary additive displays a remarkable combination of high rate and high capacity at high temperatures [8] - several factors, such as thermal stability, overcharging issue, and the extra cost of the MI additive, must be considered before considering its application in commercial products. If the outcome of such development studies is positive, MI/H_2O would be the optimal potential electrolyte additive for lithium ion battery applications.

ACKNOWLEDGEMENTS
The authors are grateful for the financial support from the National Science Council and Ministry of Economic Affairs of Taiwan, R.O.C, under grant numbers 100-2628-E-011-018-MY2, 100-2923-E-011-001-MY3, 101-3113-E-011-002, and 101-EC-17-A-08-S1-183.

References

1. M. Winter, J. O. Besenhard, M. E. Spahr, P. Novak, *Advanced Materials* 10 (1998) 725.
2. R. Koksbang, J. Barker, H. Shi, M. Y. Saidi, *Solid State Ionics* 84 (1996) 1.
3. D. Aurbach, *J. Power Sources* 68 (1997) 91.
4. S. S. Zhang, *J. Power Sources* 162 (2006) 1379.
5. T. Kawamura, S. Okada, J. Yamaki, *J. Power Sources* 156 (2006) 547.
6. U. Heider, R. Oesten, M. Jungnitz, *J. Power Sources* 81-82 (1999) 119.
7. F. M. Wang, H. M. Cheng, H. C. Wu, C. S. Cheng, *Electrochim. Acta* 54 (2009) 3344.
8. F. M. Wang, C. S. Cheng, J. Rick, *MRS Comm.* 2 (2012) 5.
9. R. Ruffo, C. Wessells, R. A. Huggins, Y. Cui, *Electrochem. Comm.* 11 (2009) 247.
10. F. M. Wang, H. Y. Wang, M. H. Yu, *J. Power Sources* 196 (2011) 10395.
11. E. Peled, D. Bar-Tow, A. Merson, A. Gladkich, L. Burstein, D. Golodnitsky, *J. Power Sources* 97-98 (2001) 52.
12. E. Peled, C. Menachem, D. Bar-Tow, A. Melman, *J. Electrochem. Soc.* 143 *(*1996) L4.
13. S. Wiatowska, V. Lair, C. Pereira-Nabais, G. Cote, P. Marcus, A. Chagnes, *Applied Surface Sci.* 257 (2011) 9110.
14. V. Eshkenazi, E. Peled, L. Burstein, D. Golodnitsky, *Solid State Ionics* 170 (2004) 83.
15. D. Aurbach, I. Weissman, A. Schechter, H. Cohen, *Langmuir* 12 (1996) 3991.
16. A. M. Andersson, K. Edstrom, *J. Electrochem. Soc.* 148 (2001) A1100.

17. L. Zhao, I. Watanabe, T. Doi, S. Okada, J. -I. Yamaki, *J. Power Sources* 161 (2006) 1275.
18. C. Moreno-Castilla, M. V. Lopez-Ramon, F. Carrasco-Marin, *Carbon* 38 (2000) 1995.
19. R. Dedryvere, S. Leroy, H. Martinez, F. Blanchard, D. Lemordant, D. Gonbeau, *J. Phys. Chem. B* 110 (2006) 12986.
20. K. I. Morigaki, A. Ohta, *J. Power Sources* 76 (1998) 159.
21. A. M. Andersson, M. Herstedt, A. Bishop, K. Edstrom, *Electrochim. Acta*, 47 (2002) 1885.
22. K. Edstrom, M. Herstedt, D. P. Abraham, *J. Power Sources* 153 (2006) 380.

© 2012 by ESG (www.electrochemsci.org)